Deep learning of genomic contexts predicts protein co-regulation and function

Yunha Hwang[1*], Andre L. Cornman[2], Sergey Ovchinnikov[3*], Peter R. Girguis[1*]

[1] Department of Organismic and Evolutionary Biology, Harvard University, Cambridge, MA, USA
[2] Independent contributor
[3] John Harvard Distinguished Science Fellowship Program, Harvard University, Cambridge, MA, USA

* co-correspondence: yhwang@g.harvard.edu, so@fas.harvard.edu, pgirguis@oeb.harvard.edu

Abstract

Deciphering the relationship between a gene and its genomic context is fundamental to understanding and engineering biological systems. Machine learning has shown promise in learning latent relationships underlying the sequence-structure-function paradigm from massive protein sequence datasets. However, to date, limited attempts have been made in extending this continuum to include higher order genomic context information. Evolutionary processes dictate the specificity of genomic contexts in which a gene is found across phylogenetic distances, and these emergent genomic patterns can be leveraged to uncover functional relationships between gene products. Here, we trained a genomic language model (gLM) on millions of metagenomic scaffolds to learn the latent functional and regulatory relationships between genes. gLM learns contextualized protein embeddings that capture the genomic context as well as the protein sequence itself, and appears to encode biologically meaningful and functionally relevant information (e.g. phylogeny, enzymatic function). Our analysis of the attention patterns demonstrates that gLM is learning co-regulated functional modules (i.e. operons). Our findings illustrate that gLM's unsupervised deep learning of the metagenomic corpus is an effective approach to encode functional semantics and regulatory syntax of genes in their genomic contexts, providing a promising avenue for uncovering complex relationships between genes in a genomic region.

Main

Introduction

Evolutionary processes result in the linkage between protein sequences, structure and function. The resulting sequence-structure-function paradigm[1] has long provided the basis for interpreting vast amounts of genomic data. Recent advances in neural network (NN)-based protein structure prediction methods[2,3], and more recently protein language models (pLMs)[4–6] suggest that data-centric approaches in unsupervised learning can represent these complex relationships shaped by evolution. To date, These models largely consider each protein as an independent and standalone entity. However, proteins are encoded in genomes, and the specific genomic context that a protein occurs in is also determined by evolutionary processes, where each gene gain, loss, duplication and transposition event is subject to selection and drift[7–9]. These processes are particularly pronounced in prokaryotic genomes where frequent horizontal gene transfers (HGT) shape genomic organization and diversity[10,11]. Thus, there exists an inherent evolutionary linkage between genomic context and gene function[12], which can be explored by characterizing patterns that emerge from large metagenomic datasets.

Recent machine learning based approaches have shown predictive power of genomic context in gene function[13] and metabolic trait evolution[14] in prokaryotic genomes. However, both these models represent genes as categorical entities, despite genes existing in continuous space, where multidimensional properties such as phylogeny, structure, and function are abstracted in their sequences. In order to close the gap between genomic-context and gene sequence-structure-function, we developed the first, to our knowledge, genomic language model (gLM) that represents proteins using pLM embeddings that have been shown to encode relational properties[4] and structure information[15]. Our model, based on the transformer[16] architecture, is trained using millions of unlabelled metagenomic sequences. We trained gLM with the masked language modeling[17] objective, with the hypothesis that its ability to attend to different parts of a multi-gene sequence will result in the learning of gene functional semantics and regulatory syntax (e.g. operons). Here, we report evidence of the learned contextualized protein embeddings and attention patterns capturing biologically relevant information. We demonstrate gLM's potential for predicting gene function and regulation, and propose future research directions, including transfer learning capabilities of gLM.

Masked language modeling of genomic sequences

Language models, such as Bidirectional Encoder Representations from Transformers (BERT[17]), learn the semantics and syntax of natural languages using unsupervised training of a large corpus. In masked language modeling, the model is tasked with reconstructing corrupted input text, where some fraction of the words are masked. Significant advances in language modeling performance was achieved by adopting the transformer[16] neural network architecture, where each token (i.e. word) is able to attend to other tokens. This is in contrast to Long-Short-Term-Memory networks (LSTMs)[18] that sequentially processes tokens with long-term dependencies. To model genomic sequences, we trained a 19-layer transformer model (**Figure 1A**) on seven million metagenomic contig fragments consisting of 15 to 30 genes from the MGnify[19] database. Each gene in a genomic sequence is represented by a 1280 feature vector (context-free protein embeddings) generated by using ESM2 pLM[15], concatenated with an orientation feature (forward or backward). For each sequence, 15% of genes are randomly masked, and the model learns to predict the masked label using the context. Based on the insight that more than one gene can legitimately be found in a particular genomic context, we allow the model to make four different predictions and also predict their associated probabilities. Thus, instead of predicting their mean value, the model can approximate the underlying distribution of multiple genes that can occupy a genomic niche We assess the model's performance using a pseudo-accuracy metric, where a prediction is considered correct if it is closest to the masked protein in euclidean distance compared to the other proteins encoded in the sequence (see methods). We validate our model's performance on the *Escherichia coli* K-12 genome[20] by excluding from training 5.1% of MGnify subcontigs where more than half of the proteins are similar (>70% sequence identity) to *E. coli* K-12 proteins. It is important to note that our goal was not to remove all *E. coli* K-12 homologs from the training, which would have removed a vast majority of training data as many essential genes are shared

across organisms. Instead, our goal was to remove as many *E.coli* K-12-like genomic contexts (subcontigs) from training, which is more appropriate for the training objective. gLM achieves 71.9% in validation pseudo-accuracy and 59.2% in validation absolute accuracy (**Extended Data 1)**. We baseline our performance with a bidirectional LSTM model trained using the same language modeling task on the same training dataset, where validation performance plateaus at 28% pseudo-accuracy and 15% absolute accuracy (**Extended Data 1 and 2**).

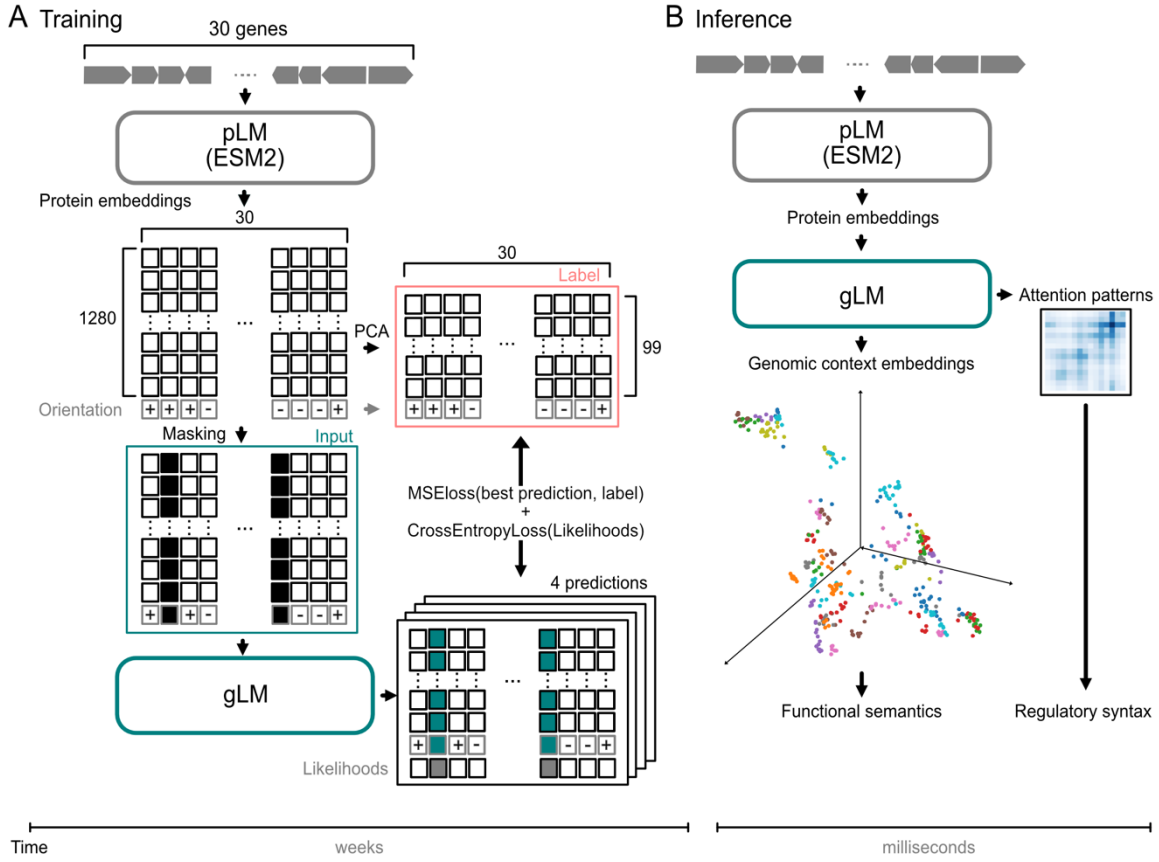

Figure 1. gLM training and inference schematics. A) Training begins with converting 15-30 gene metagenomic subcontigs to protein embeddings using ESM2. Orientation feature is concatenated for each protein and 15% of the proteins are masked randomly to generate training inputs. Labels are generated by applying PCA dimensionality reduction on the ESM2 protein embeddings, and concatenating the orientation feature. gLM is trained to make four possible predictions for the masked tokens, and their associated likelihoods. Training loss is calculated on both the prediction and likelihoods. The training stage takes several weeks on four NVIDIA A100 GPUs. B) At inference time, inputs are generated from a metagenomic subcontig using ESM2 output concatenated with an orientation feature. Hidden states and attention patterns of the trained gLM can be used for various downstream tasks.

Contextualized gene embeddings capture gene semantics

The mapping from gene to gene-function in organisms is not one-to-one. Similar to words in natural language, a gene can confer many different functions[21] depending on its context[22], and many genes can confer similar functions (i.e. convergent evolution[23], remote homology[24]). We used gLM to generate 1280-feature contextualized protein embeddings at inference time (**Figure 1B**), and we examined the "semantic" information captured in these embeddings. Analogous to how words are likely to have different meanings depending on the type of text in which they are found (**Figure 2A)**, we find that contextualized protein embeddings of genes that appear across multiple environments (biomes) tend to cluster based on biome types. For instance, a gene encoding a protein annotated "translation initiation factor IF-1" occurs multiple times across biomes. While the context-free protein embedding (ESM2 output) is identical across all occurrences (**Figure 2B)**, its contextualized embeddings cluster with biome types (**Figure 2C**). This suggests that the diverse genomic contexts that a gene occupies are specific for different biomes, implying biome-specific gene semantics.

We further explored an ecologically important example of genomic "polysemy" (multiple meanings conferred by the same word) of methyl-coenzyme M reductase (MCR) complex. The MCR complex is able to carry out a reversible reaction (Reaction 1 in **Figure 2G**), whereby the forward reaction results in the production of methane (methanogenesis) while the reverse results in methane oxidation (methanotrophy). We first examine the McrA (methyl-coenzyme M reductase subunit alpha) protein in diverse lineages of ANME (ANaerobic MEthane oxidizing) and methanogenic archaeal genomes. These archaea are polyphyletic and occupy specific ecological niches. Notably, similar to how a semantic meaning of a word exists on a spectrum and a word can have multiple semantically appropriate meanings in a context (**Figure 2D),** the MCR complex can confer different functions depending on the context. Previous reports demonstrate capacities of ANME (ANME-2 in particular) carrying out methanogenesis[25] and methanogens conducting methane oxidation in specific growth conditions[26]. The context-free ESM2 embedding of these proteins (**Figure 2E**) shows little organization, with little separation between ANME-1 and ANME-2 McrA proteins. However, contextualized gLM embeddings (**Figure 2F**) of the McrA proteins show distinct organization where ANME-1 McrA proteins form a tight cluster, while ANME-2 McrA proteins form a cluster closer to methanogens. This organization reflects the phylogenetic relationships between the organisms that McrAs are found in, and reflect distinct operonic and structural divergence of MCR complexes in ANME-1 compared to those found in ANME-2 and methanogens[27]. As proposed by Shao et al.[27], the preferred directionality in Reaction 1 (**Figure 2G**) in ANME-2 and some methanogens may be more dependent on thermodynamics.

We also demonstrate that contextualized gLM embeddings are more suitable for determining the functional relationship between gene classes. Analogous to how the words "dog" and "cat" are closer in meaning relative to "dog" and "train" (**Figure 2H)**, we see a pattern where Cas1 and Cas2 that appear diffuse in multiple subclusters in context-free protein embedding space (**Figure 2I)** cluster in contextualized embedding space (**Figure 2J**). This reflects their similarity in function (e.g. phage defense). This is also demonstrated in biosynthetic genes, lipopolysaccharide synthase (LPS) and polyketide synthase (PKS) genes clustering closer together in contextualized embedding space distinct from the Cas proteins (**Figure 2J)**. Contextualized protein embeddings are therefore able to capture relational properties semantic information[28], where proteins that are more similar in their function appear in more similar genomic contexts.

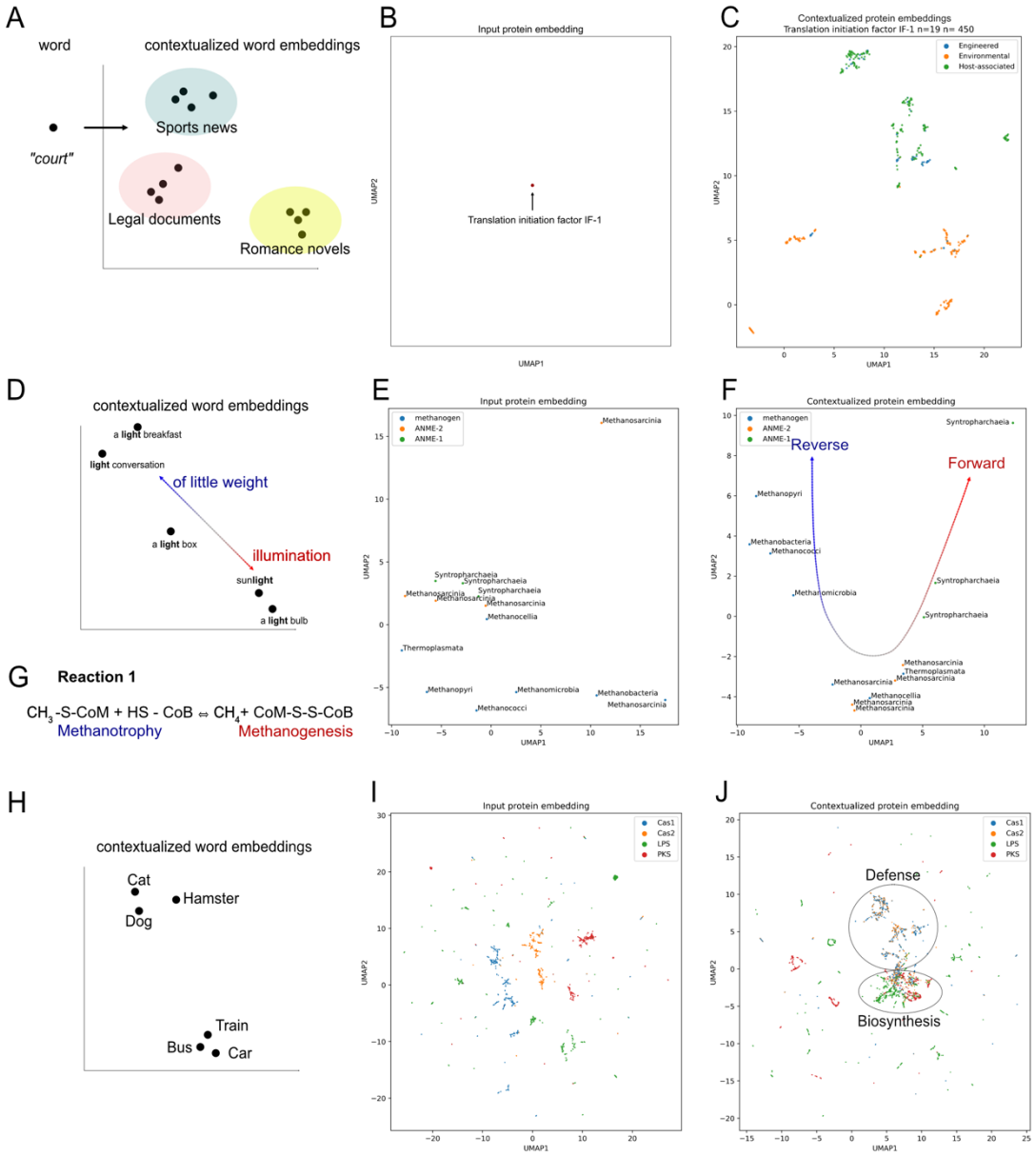

Figure 2. Contextualized protein embedding analysis and comparison with concepts in natural language modeling. A) A word upon contextualization can be mapped to embedding space. For many words, the semantic meaning varies in different types of literature, and therefore their contextualized embeddings cluster with source text type. Figure was created for qualitative visualization. B) The input protein embedding (output of ESM2 and context-free protein embedding) is the same across all occurrences of the protein in the database. C) Contextualized protein embeddings of the same protein (last hidden layer of gLM at inference time) cluster with biome type, analogous to the source text type in natural language (A). D) A word's meaning upon contextualization varies across a continuous spectrum and can be ambiguous even with contextualization (e.g. double entendre). E) Input protein embeddings of McrA sequences in genomes, colored by metabolic classification of the organism (ANME, methanogen) based on previous studies and labeled by class-level taxonomy. F) Clustering of McrA sequences upon contextualization, with the likelihoods in the direction of Reaction 1 that the MCR complex carries out. G) Reaction 1, carried out by the MCR complex, either backward (Methanotrophy) or forward (Methanogenesis). H) Geometric relationship between contextualized protein embeddings based on the semantic closeness of words. I) Input (context-free) protein embeddings of Cas1, Cas2, lipopolysaccharide

159 synthases (LPS) and polyketide synthases (PKS) showing clustering based on structural and sequence
160 similarity. J) Clustering of contextualized protein embeddings where phage defense proteins cluster (Cas1
161 and Cas2) and biosynthetic gene products cluster (LPS and PKS).
162

Characterizing the unknown

Metagenomic sequences feature many genes with unknown or generic functions, and some are so divergent that they do not contain sufficient sequence similarity to the annotated fraction of the database[29]. In our dataset, of the 30.8M protein sequences, 19.8% could not be associated with any known annotation (see methods), and 27.5% could not be associated with any known Pfam domains using a recent deep learning approach (ProtENN[30]). Understanding the functional role of these proteins in their organismal and environmental contexts remains a major challenge because most of the organisms that house such proteins are difficult to culture and laboratory validation is often low-throughput. We demonstrate the potential of using contextualized protein embeddings to assign putative functions to previously unannotated proteins. This approach is motivated by the observation that proteins that confer similar functions are found in similar genomic contexts due to selective pressures bestowed by functional relationships (e.g. protein-protein interactions, co-regulations) between genes. pLM-based context-free protein embeddings have previously been proposed for annotation transfer[31], particularly through remote homology detection[4]. However, we find that many of these unannotated proteins often do not cluster with proteins with known function when using context-free pLM embeddings (**Figure 3A**). In contrast, by using gLM-based contextualized protein embeddings, more unannotated proteins can be associated with proteins with functional annotation, resulting in higher annotation transfer potential (**Figure 3B**).

Contextualization improves enzyme function prediction

To test the hypothesis that the genomic context of the protein can be used to aid function prediction, we compared how much the addition of context information can improve the expressiveness of protein representations for enzyme function prediction. Specifically, we examined the capabilities of context-free (pLM) representation and context-added (pLM+gLM) representations in classifying enzyme commission (EC)[32] numbers of proteins. We trained a simple three-layer perceptron neural network (**Extended Data 3**) to predict all four hierarchies of EC number on a random 100,000 subcontigs in the training database, from which 115768 unique MGYPs could be assigned to 2637 different EC numbers (see methods). We find 2% and 3% increases in test prediction accuracy and precision respectively with the addition of contextualization (**Extended Data 4**). We found that the addition of context information results in largest performance (F1 score) gains (up to six-fold) in some EC classes that are known to feature structural diversity and phylogenetic heterogeneity (**Figure 3C**). For instance, EC 1.6.5.11 designates NADH:quinone oxidoreductases, which consists of structurally diverse enzymes with various substrate binding sites grouped together by the specific function of catalyzing electron transfer from NAD(P)H to quinones[33]. Similarly, ECs 2.7.7.65 and 2.7.11.1, denoting diguanylate cyclases and non-specific serine/threonine protein kinases respectively, feature diversity in substrates that they can bind[34,35]. In some EC classes, however, the additional context information seems to lower the prediction performance. For instance, ECs 4.1.1.81 and 5.4.99.60 designate pyridoxal-phosphate protein and cobalt-precorrin-8 methylmutase respectively, which are structurally and evolutionarily conserved[36]. We also find that the additional context information leads to worse performance for pyruvate synthases (EC 1.2.7.1) suggesting the possibility that the diverse contexts that pyruvate synthases are found in may result in misclassification or conversely represent possible functional diversity[37]. Previous studies[37–39] have utilized deep learning to predict EC numbers directly from protein sequences and fine-tuning such approaches with contextualization could provide ways to infer function even for classes with fewer training examples or identify proteins with more than one function.

Horizontal transfer frequency corresponds to genomic context embedding variance

A key process that shapes microbial genome organization and evolution is horizontal gene transfer (HGT). The taxonomic range in which genes are distributed across the tree of life depends on their function and the selective advantage they incur in different environments. Relatively little is known about the specificity in the genomic region into which a gene gets transferred across phylogenetic distances. We examined the variance of genomic context embeddings for proteins that occur at least one hundred times in the database. Variance of genomic contexts are calculated by taking a random sample of 100 occurrences and then

calculating the mean pairwise distances between the hundred contextualized protein embeddings. We conduct such independent random sampling and distance calculation ten times per protein and then calculate the mean value and term this the genomic context variance. Our results show that the genomic context variances are log-normally distributed for both annotated and unannotated fractions of the genes **(Figure 3D)**. The most context-variant proteins in the right tail included phage proteins and transposases, reflecting their ability to self-mobilize. Genomic context variances can be used as a proxy for horizontal transfer frequencies and can be used to compare the fitness effects of the genomic context on the evolutionary trajectory (e.g. gene flow) of genes.

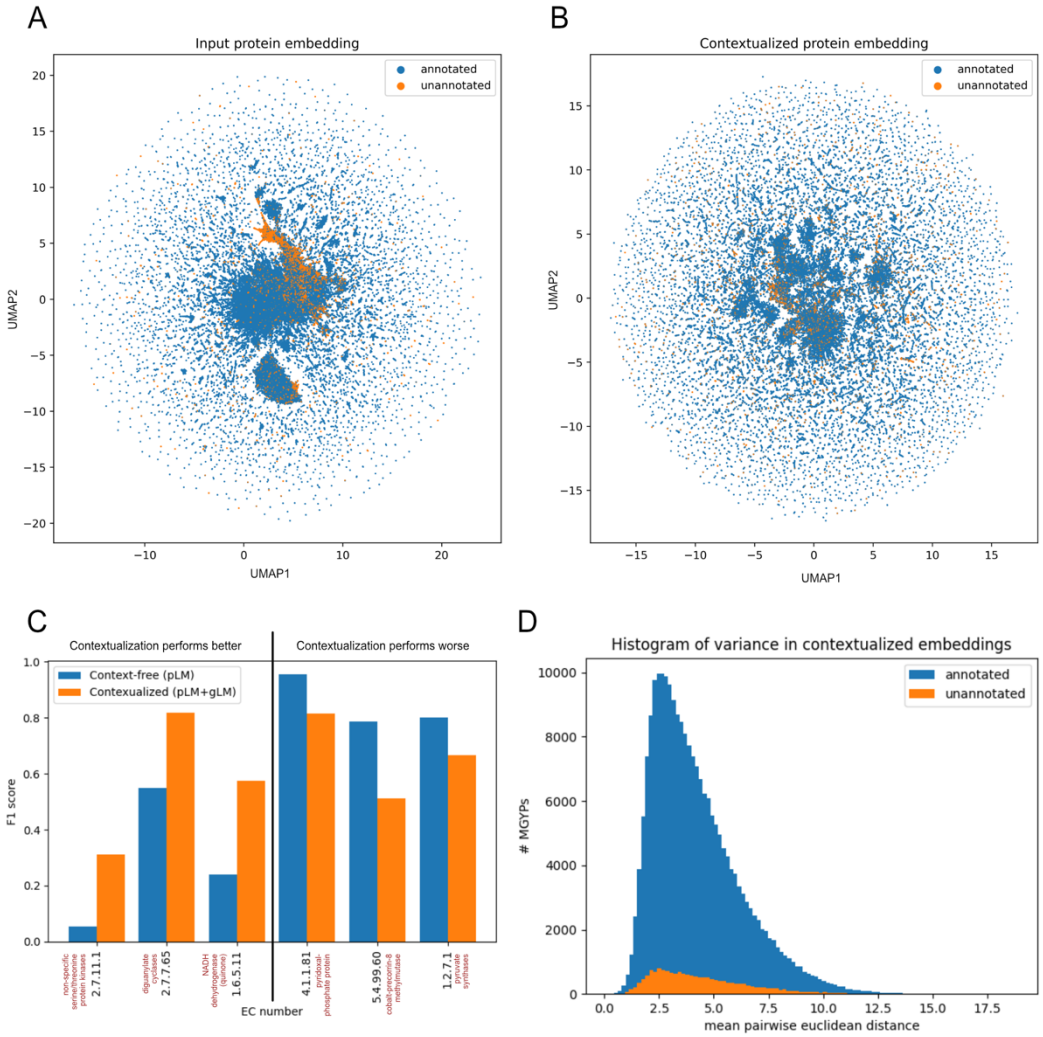

Figure 3. Contextualization of unannotated proteins. A) UMAP visualization of input protein embeddings (ESM2 output) of annotated proteins (blue) and proteins without annotation (orange) from a random 0.15% subset of the MGnify database. B) UMAP visualization of contextualized embeddings of the same proteins across their occurrences in the 0.15% subset of the MGnify database. C) three classes with highest performance gain in EC prediction with contextualization (left) and three where contextualization results in diminished performance (right) D) Histogram of variance (# bins = 100) in contextualized embeddings of MGYPs that occur at least 100 times in the database. Histograms for unannotated and annotated fraction of the MGYPs are plotted separately and bars are not stacked.

Transformer's attention captures operons

The transformer attention mechanism[16] models pairwise interaction between different tokens in the input sequence. Previous examinations of the attention patterns of transformer models in natural language processing (NLP)[40] have suggested that different heads appear to specialize in syntactic functions. Subsequently, different attention heads in pLMs[41] have been shown to correlate to specific structural elements and functional sites in a protein. For our gLM, we hypothesized that specific attention heads focus on learning operons, a "syntactic" feature in genomes where multiple genes form regulatory modules. We used the E.coli K-12 operon database[42] consisting of 817 operons for validation. gLM contains 190 attention heads across 19 layers. We found that heads in shallower layers correlated more with operons (**Figure 4A, Extended Data 5)**, with raw attention scores in the 7th head of the 2th layer [L2-H7] linearly correlating with operons with 0.44 correlation coefficient (Pearson's rho, Bonferroni adjusted p-value < 1E-5) (**Figure 4B**). We further trained a logistic regression classifier using all attention patterns across all heads. This classifier predicted the presence of an operonic relationship between a pair of proteins in a sequence with mean average precision of 0.77 (**Figure 4C**).

gLM predicts paralogy in protein-protein interactions

Proteins in an organism are found in complexes and interact physically with each other. Recent advances in protein-protein interaction (PPI) prediction and structural complex research has largely been guided by identifying interologs (conserved PPI across organisms) and co-evolutionary signals between residues [43]. However, distinguishing paralogs from orthologs (or the "Paralog matching" problem) in the expanding sequence dataset remains a computational challenge requiring queries across the entire database and/or phylogenetic profiling, and in cases where multiple interacting pairs are found within an organism (eg. histidine kinases (HK) and response regulators (RR)), prediction of interacting pairs is particularly difficult[44]. We reasoned that gLM, although not directly trained for this task, may have learned the relationships between paralogs versus orthologs. In order to test this capability, we used a well studied example of interacting paralogs (ModC and ModA, **Figure 4D**) which form an ABC transporter complex. We queried gLM to predict the embedding of an interacting pair given no context except the protein sequence of either ModA or ModC. We find that without any fine-tuning gLM performs better than what is expected by random chance (see methods). Specifically, for 417 out of 2700 interacting pairs, gLM is able to make predictions that are belong to the same cluster (50% sequence identity, n=2100 clusters) as the true label, and in 73 out of 2700 interacting pairs, the gLM predicts a label that is closest to the exact interacting pair (**Figure 4E)**. Importantly, when paralogs are correctly paired, gLM is very certain about the prediction (average confidence = 0.79), while less certain predictions are either out of distribution, or closer to the mean of labels (**Figure 4F**). We attribute part of the inaccuracies in prediction due to the fact that gLM was not trained on the task of predicting a masked gene given only a single gene as genomic context, and we expect the performance to improve with expanding the training sequence length range and fine-tuning the model specifically for the "paralog matching" problem.

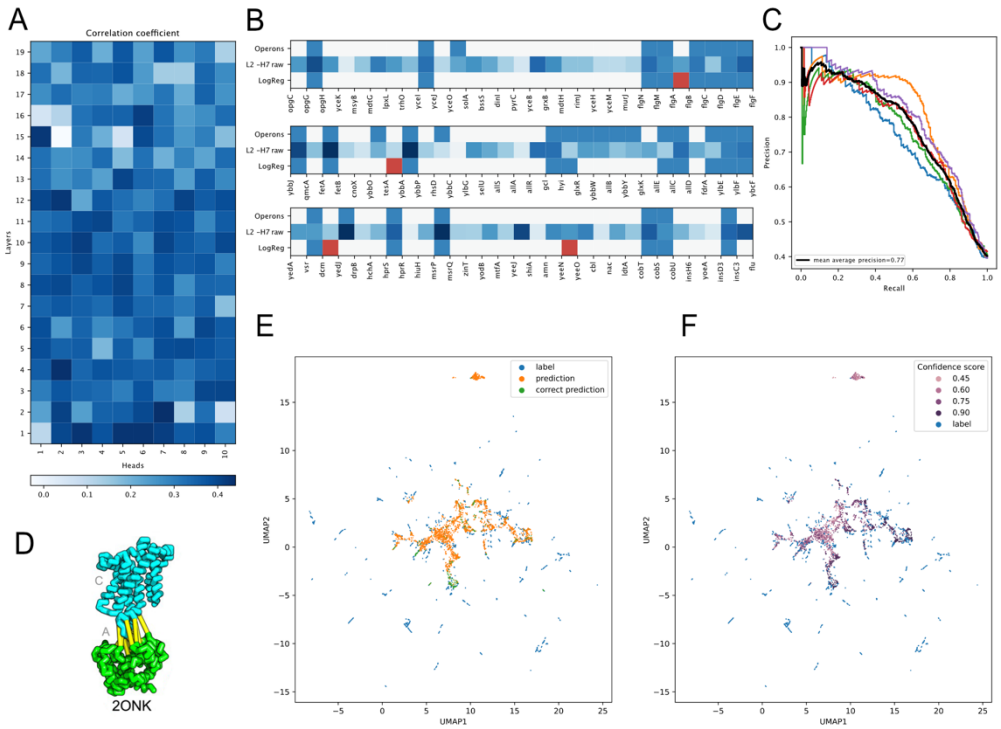

Figure 4. Attention analysis. A) Correlation coefficients (Pearson's rho) between attention heads across layers and operons. B) Three random examples of ground truth operons (top row), raw attention scores (middle row) between neighboring proteins in the highest correlating attention head and logistic regression prediction using all attention heads (last row) where false positive predictions are marked in red. C) Cross-validation precision-recall curve of logistic regression trained using all operons and attention heads. D) ModA and ModC interaction (adapted with permission from Ovchinnikov et al.[43]) E) Projection of predictions (orange) and labels (blues) of paralogs, where correct predictions are colored in green. F) Predictions are colored based on the confidence with which it was predicted.

Contextualized contig embeddings and potential for transfer learning

Contextualized protein embeddings encode the relationship between a specific protein and its genomic context, retaining the sequential information within a contig. We hypothesized that this contextualization adds biologically meaningful information that can be utilized for further characterization of the multi-gene genomic contigs. Here, we define a contextualized contig embedding as a mean-pooled hidden layer across all proteins in sequence, and a context-free contig embedding as mean-pooled ESM2 protein embeddings across the sequence (see methods). Both embeddings consist of 1280 features. We test our hypothesis by examining each of these embeddings' ability to linearly distinguish viral sequences from prokaryotic (bacterial and archaeal) sub-contigs. In metagenomic datasets, the taxonomic identity of assembled sequences must be inferred post-hoc, therefore the identification of viral sequences is conducted based on the presence of viral genes and viral genomic signatures[45]. However, such classification task remains a challenge particularly for smaller contig fragments and less characterized viral sequences. Here, we sampled random 30-protein sub-contigs from the representative prokaryotic genome database and reference viral genomes in the NCBI and visualized their context-free contig embeddings (**Figures 5AC**) and contextualized contig embeddings (**Figures 5BD**). We observed more separation and taxonomic clusters at both domain- (**Figures 5AB)** and class-levels (**Figures 5CD)**, suggesting that taxonomic signature is enhanced by encoding the latent relationships between proteins. This is further validated by training a logistic regression classifier on context-free and contexutalized contig embeddings for class-level taxonomy, where we see a 3% improvement in average precision (**Figures 5EF**). This emphasizes the biological importance of a protein's relative position in the genome and its relationship with the genomic environment, and further indicates that this information can be effectively encoded using gLM. Contextualized contig embeddings present opportunities for transfer learning beyond viral sequence prediction, such as improved metagenomically-assembled genome (MAG) binning and assembly correction.

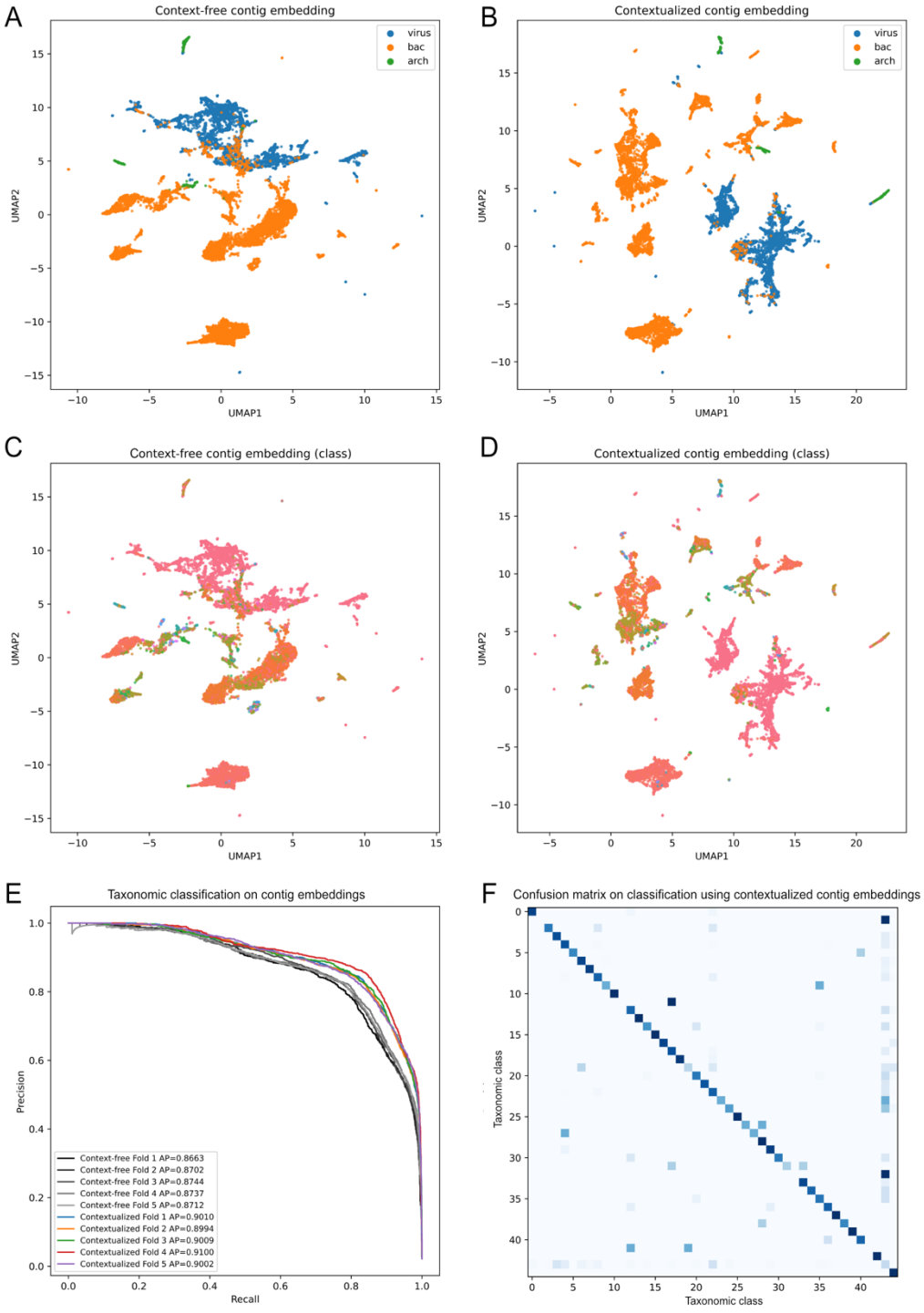

Figure 5. Taxonomic classification using context-free and contextualized contig embeddings. Random 30-gene contigs from representative prokaryotic genomes and reference viral genomes were embedded by mean-pooling ESM2 protein embeddings (context-free contig embeddings) and by mean-pooling the last hidden layer of gLM (contextualized contig embeddings). UMAP visualization of context-free contig embeddings colored by the domain (A) and class (C) and contexutalized contig embeddings colored by the domain (B) and class (D). E) Micro-averaged precision-recall curves and average precisions for logistic regression classifiers trained using context-free contig embeddings (grey lines) and contextualized contig

311 embeddings (color lines) for class-level taxonomy classification task. Each line represents a fold in stratified
312 k-fold cross-validation (k=5). F) Confusion matrix for logistic regression classifier trained on
313 contextualized contig embeddings; taxonomic classification at class-level.

Discussion

The unprecedented amount and diversity of metagenomic data, coupled with advances in deep learning presents an exciting opportunity for building a large computational model that can learn hidden patterns and structures of biological systems. Such a model builds upon the conceptual and statistical frameworks that evolutionary biologists have developed for the past century. With capabilities of abstracting much larger amounts of data, it may bring us closer to understanding the extraordinary complexity of organismal genomes and their encoded functions. The work presented here demonstrates the concept of genomic language modeling. Our implementation of the masked genomic language modeling illustrates the feasibility of training, evidence of biological information being captured in learned contextualized embeddings, and meaningful interpretability of the attention patterns. We propose the following key directions for future works: First, the transformer architecture has shown to be successful in efficient scaling; in both natural language[46] and protein language processing[15], increasing the number of parameters in the model along with the training dataset size have been shown to lead to vastly improved performance and generalizability. Our model consists of ~1B parameters which is at least a magnitude smaller compared to state-of-the-art pLMs. With further hyperparameter tuning and scaling, we expect better performance of the model. Second, our model currently uses protein-level pLM embeddings to represent proteins in the input. These embeddings are generated by mean-pooling the residue-level hidden states across the protein sequence, and therefore the residue specific information is likely obscured. Future approaches for scaling should consider using the residue-level embeddings, which contain richer information that can be used to link residue-to-residue co-evolutionary interactions between proteins. Third, the task of reconstructing masked protein embeddings requires modeling a distribution over possible embeddings; our method approximates this distribution using a fixed number of predictions. Future work could improve upon this by using a generative approach, such as a diffusion or GAN model. This may allow for better prediction accuracy and greater generalizability for unseen datasets. Fourth, adding non-protein modalities (e.g. non-coding regulatory elements[13]) as input to gLM may also greatly improve gLM's representation of biological sequence data, and can learn protein function and regulation conditioned upon other modalities[47].

One of the most powerful aspects of the transformer-based language models is their potential for transfer learning and fine-tuning. Here, we tested some of the capabilities of gLM and successfully showed that higher order biological information including gene function and regulation can be learned using genomic sequences. Our results highlight the importance of contextualization of biological data, particularly as we scale our modeling efforts from biomolecules to whole organisms. We propose the following promising future directions for applying gLM for advancing biological research. 1) Feature-based transfer learning for predicting protein function (e.g. Gene Ontology [GO] term, EC number), particularly those with limited sequence and structural homology. 2) Fine-tuning gLM for the protein-protein-interactome prediction task. 3) Using gLM features to encode genomic contexts as additional input for improved and contextualized protein structure predictions. Taken together, genomic language modeling is a promising methodology to condense important biological information from full metagenomic sequences. Coupled with the advances in long-read sequencing, we expect a drastic increase in the input data quality, quantity and diversity. Genomic language modeling presents an avenue to bridge the gap between atomic structure and organismal function, and thereby bringing us closer to genomically engineering organisms.

Methods

Sequence database

The genomic corpus was generated using the MGnify[19] dataset (released 2022-05-06 and downloaded 2022-06-07). First, genomic contigs with greater than 30 genes were divided into 30 gene non-overlapping subcontigs resulting in a total of 7.324.684 subcontigs with lengths between 15 and 30 genes (subcontigs < 15 genes in length were removed from the dataset). Each gene in the subcontig was mapped to a representative protein sequence (rep-MGYP) using mmseqs/linclust[48], with coverage and sequence identity thresholds set at 90% (pre-computed in the MGnify database), resulting in a total of 30,800,563 representative MGYPs. Each rep-MGYP was represented by a 1280-feature protein embedding, generated by mean-pooling the last hidden layer of the ESM2[49] "esm2_t33_650M_UR50D" model. Due to the memory limitation in computing embeddings for very long sequences, 116 of the MGYP sequences longer than 12290 amino acids were truncated to 12290 amino acids. ESM2 embeddings were subsequently standardized and clipped at (-10,10). A small fraction (0.4%) of the genes could not be mapped to a representative MGYP and therefore the corresponding sequence information could not be retrieved from the MGnify server; these sequences were assigned a 1280 feature vector of ones. For each gene in the sub-sequence, we added a gene orientation feature to the standardized MGYP protein embedding, where 0.5 denotes "forward" orientation relative to the direction of sequencing, and -0.5 denotes "reverse" orientation. Thus, each gene was represented by a 1281 feature vector in our corpus.

gLM architecture and training

gLM was built on the huggingface implementation of the RoBERTa[50] transformer architecture. gLM consisted of 19 layers with hidden size 1280 and ten attention heads per layer, with relative position embedding ("relative_key_query")[51]. For training, 15% of the tokens (genes) in the sequence (subcontig) were randomly masked to a value of -1. We then tasked the model with the objective of predicting the label of the masked token, where the label consists of a 100-feature vector that consists of the PCA whitened 99 principal components of the corresponding ESM2 protein embedding concatenated with its orientation feature. Specifically, gLM projects the last hidden state of the model into four 100-feature vectors and four corresponding likelihood values using a linear layer. Total loss is calculated using the following equation:

$$MSE(closest\ prediction, label) + \alpha * CrossEntropyLoss(likelihoods, closest\ prediction\ index)$$

by summing the mean squared error between the closest prediction to the label and summing it with α*cross entropy loss between the likelihoods and the closest prediction, where α = 1e-4. gLM was trained in half precision with batch size 3000 with distributed data parallelization on four NVIDIA A100 GPUs over 1296960 steps (560 epochs) including 5000 warm-up steps to reach a learning rate of 1e-4 with AdamW[52] optimizer.

Performance metric and validation

In order to evaluate the model quality and its generalizability beyond the training dataset, we use a pseudo-accuracy metric, where we deem a prediction to be "correct" if it is closest in euclidean distance to the label of the masked gene relative to the other genes in the subcontig. Thus, $pseudo\ accuracy = \frac{\#\,count(argmin(dist(prediction, labels\ in\ subcontig)) == index(masked\ gene))}{\#\,masked\ genes}$. We chose to validate our metric and subsequent analyses on the best annotated genome to date: E.coli K12[53]. In order to remove as many *E.coli* K12 like subcontigs from the training dataset, we removed 5.2% of the subcontigs in which more than half of the genes were > 70% similar (calculated using mmseqs2 search[48]) in amino acid sequence to *E.coli* K12 genes. We validate our pseudo accuracy metric by calculating the absolute accuracy on the *E.coli* K12 genome for which each gene was masked sequentially: $absolute\ accuracy = \frac{\#\,count(argmin(dist(prediction, all\ genes\ in\ E.coli\ K12)) == index(masked\ gene))}{\#\,genes\ in\ E.coli\ K12}$

Contextualized embedding calculation and visualization

Contextualized gene embeddings of a gene by first inputting a 15-30 gene subcontig containing the gene of interest, and then running inference on the subcontig using the trained gLM without masking. We then use the last hidden layer of the model corresponding to the gene as the embedding consisting of 1280 features.

Gene annotation

Genes were annotated using Diamond v2.0.7.145[54] against the UniRef100 database[55] with an e-value cut-off 1E-5. Genes were labeled as "unannotated" if either 1) no match was found in the UniRef100 database, or 2) the match was annotated with following keywords: "unannotated", "uncharacterized", "hypothetical", "DUF"(domain of unknown function).

McrA protein analysis

McrA protein encoding Methanogens and ANME genomes were selected from the accession ID list found in the supplement of Shao et al[27]. Sub-contigs containing *mcrA* were extracted with at most 15 genes before and after *mcrA* and the context-free and contextualized embeddings of McrA was calculated using the ESM2 and gLM respectively.

Enzyme Commission number prediction

Enzyme Commission (EC) numbers were assigned to MGYPs by searching against the "KNN dataset" DeepRe using mmseqs2[48]. Approximately 18% of the MGYPs could be assigned an EC number. We then selected a random set of 100,000 subcontigs from the MGnify training data. First occurrences of MGYPs with EC number were encoded into context-free (pLM) embeddings, using ESM2 mean-pooled last hidden layer. Context-added (pLM+gLM) embeddings are generated by running gLM inference on the subcontig, and then concatenating the pLM embedding with the last hidden layer of gLM corresponding to that MGYP. We remove redundancies by making sure each data point consists of a unique MGYP. EC classes where not all four numbers are assigned (e.g. 1.2.3._.) are removed from the dataset. All EC classes with less than 3 data points are removed, and subsequently split into train, validation and test sets with 0.72/0.08/0.2 split, with stratification on labels. A three layer perceptron (**Extended Data 3**) is trained with ReLu activation, batch normalization, and 0.2 dropout; EC number prediction is made upon softmax of the final layer.

Variance of contextualized protein embedding analysis

Contextualized protein embeddings are generated at inference time. Variances of contextualized protein embeddings were calculated for MGYPs that occur at least 100 times in the dataset, excluding the occurrences at the edges of the subcontig (first or last token). For each such MGYP, we take 10 random independent samples consisting of 100 occurrences and calculate the mean pairwise euclidean distances between the contextualized embeddings.

Attention analysis

Attention heads (n = 190) were extracted by running inference on unmasked subcontigs, and the raw attention weights were subsequently symmetrized. *E.coli* K12 RegulonDB[53] was used to probe heads with attention patterns that correspond the most with operons. Pearson's correlation between symmetrized raw attentions and operons were calculated for each head. We trained a logistic regression classifier that predicts whether two neighboring genes belong to the same operon based on the attention weights across all attention heads corresponding to the gene pair.

Paralogy and orthology analysis

UniProt IDs from ABC transporter ModA and ModC protein interacting paralog pairs (n = 4823) were previously identified by Ovchinnikov et al[43] and were downloaded from https://gremlin.bakerlab.org/cplx.php?uni_a=2ONK_A&uni_b=2ONK_C and subsequently used to download raw protein sequences from the UniProt server. Only pairs (n = 2700) where both raw sequences were available for download, and where the UniProt ID differed by one (indicating adjacent positioning in the reference genome) were selected for subsequent analyses. We constructed test contigs consisting of

three genes, where first and third genes are masked, and the second gene encodes one of the pair in forward direction. We then queried gLM to predict the two neighboring masked genes, and considered the prediction to be "exactly correct" if either of the masked genes's highest confidence predicted label is closest to the label of the interacting protein compared to the orthologs. A prediction is considered "correct" if the label closest to the highest confidence prediction belongs to the same sequence cluster (50% amino acid sequence identity, calculated using CD-HIT[56]). Random chance "correct" prediction rate was simulated using 1000 iterations of random predictions generated within the standard normal distribution and comparing them against the label embeddings from the interacting paralogs dataset.

Taxonomic analysis and visualization

4551 bacterial and archeal representative genomes and 11660 reference viral genomes were downloaded from the RefSeq database (ftp://ftp.ncbi.nlm.nih.gov/genomes/refseq) on 12 Feb 2023. A random 30-gene sub-contig is chosen and encoded using ESM2, which then were subsequently concatenated with an orientation vector and then used as input for the trained gLM. The last hidden layer was mean-pooled across the sequence to retrieve 1280-feature contextualized contig embeddings. The ESM2 output protein embeddings were also mean-pooled across the sequence to retrieve 1280-feature context-free contig embeddings. We trained a logistic regression classifier to predict the class-level taxonomy of subcontigs and evaluated the performance using stratified k-fold cross-validation (k=5).

Data and code availability

Data availability

Training dataset is available for download from the MGnify server (http://ftp.ebi.ac.uk/pub/databases/metagenomics/peptide_database/).

Code availability

Training and inference code is available at https://github.com/y-hwang/gLM

Declarations

Acknowledgements. We would like to thank the EBI MGnify team for generating and maintaining the metagenome database. We would also like to thank Meta AI's ESM developers who made both the folded MGnify proteins structures and source-code openly available. We also thank Simon Roux and Landen Goszashti for insightful discussions.

Author contributions. YH prepared the datasets and trained the model with support from ALC and SO; ALC, SO and PRG provided input in analysis and data interpretation; YH wrote the manuscript with input from all authors; All authors read and approved the final manuscript.

Funding information. This work was supported by the Gordon and Betty Moore Foundation grant #9208 to P.R.G., NSF OCE-1635365 to P.R.G, and by the National Aeronautics and Space Administration under grant no. 80NSSC18K1140 and 80NSSC19K1427 issued through the NASA Network for Life Detection program to P.R.G. The computations in this paper were run on the FASRC Cannon cluster supported by the FAS Division of Science Research Computing Group at Harvard University.

Conflicting interests. The authors declare that they have no conflict of interest.

Extended data

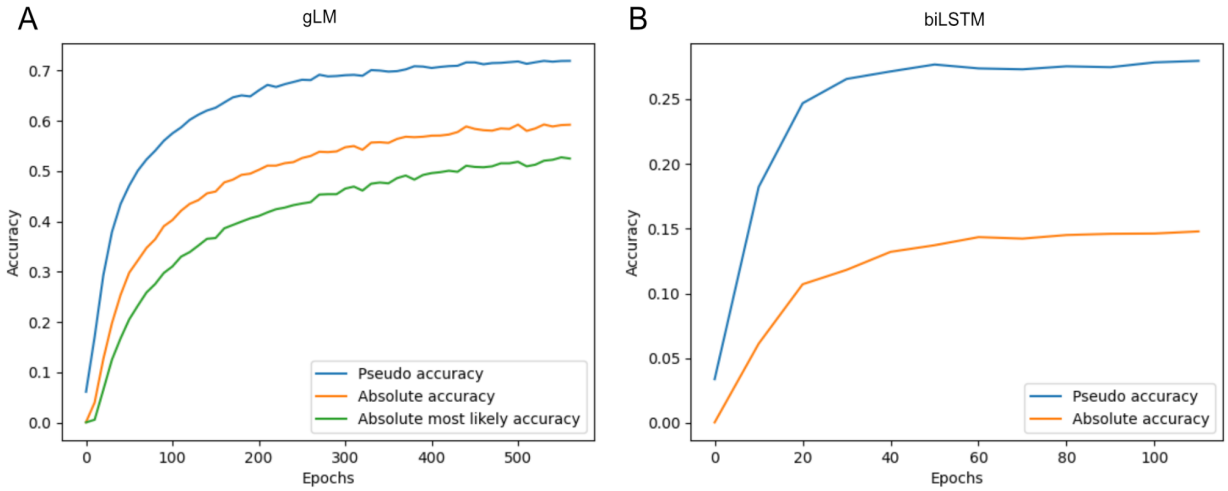

Extended data 1. Validation accuracy curves for gLM (A) and biLSTM baseline (B).

Extended data 2. Comparison of biLSTM baseline model with transformer-based gLM architecture and validation performances.

	biLSTM	gLM
Number of layers	5	19
Attention heads	N/A	20
Input embedding dimension	1281	1281
Hidden size	1280	1280
Batch size	4000	3000
Learning rate	1e-4	1e-4
Warm up steps	5000	5000
Training steps	1	1296960
Number of predictions	1	4
Number of parameters	27811840	954736916
Pseudo-accuracy (validation)	27.9	71.9
Absolute accuracy (validation)	14.78	59.2

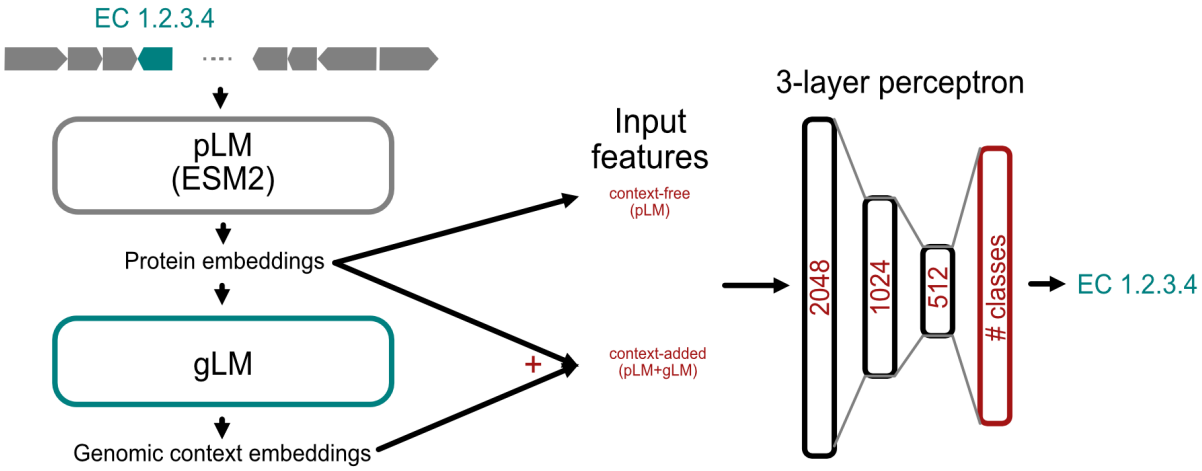

Extended Data 3. EC number prediction using a three-layer perceptron.

Extended data 4. EC number prediction perceptron results.

	Context-free representation (pLM)	Contextualized representation (gLM+pLM)
Validation accuracy	0.85	0.875
Test accuracy	0.850	0.868
Test mean average precision ("micro"-average)	0.725	0.757
Number of training epochs until peak validation accuracy (point of early stopping)	65	80

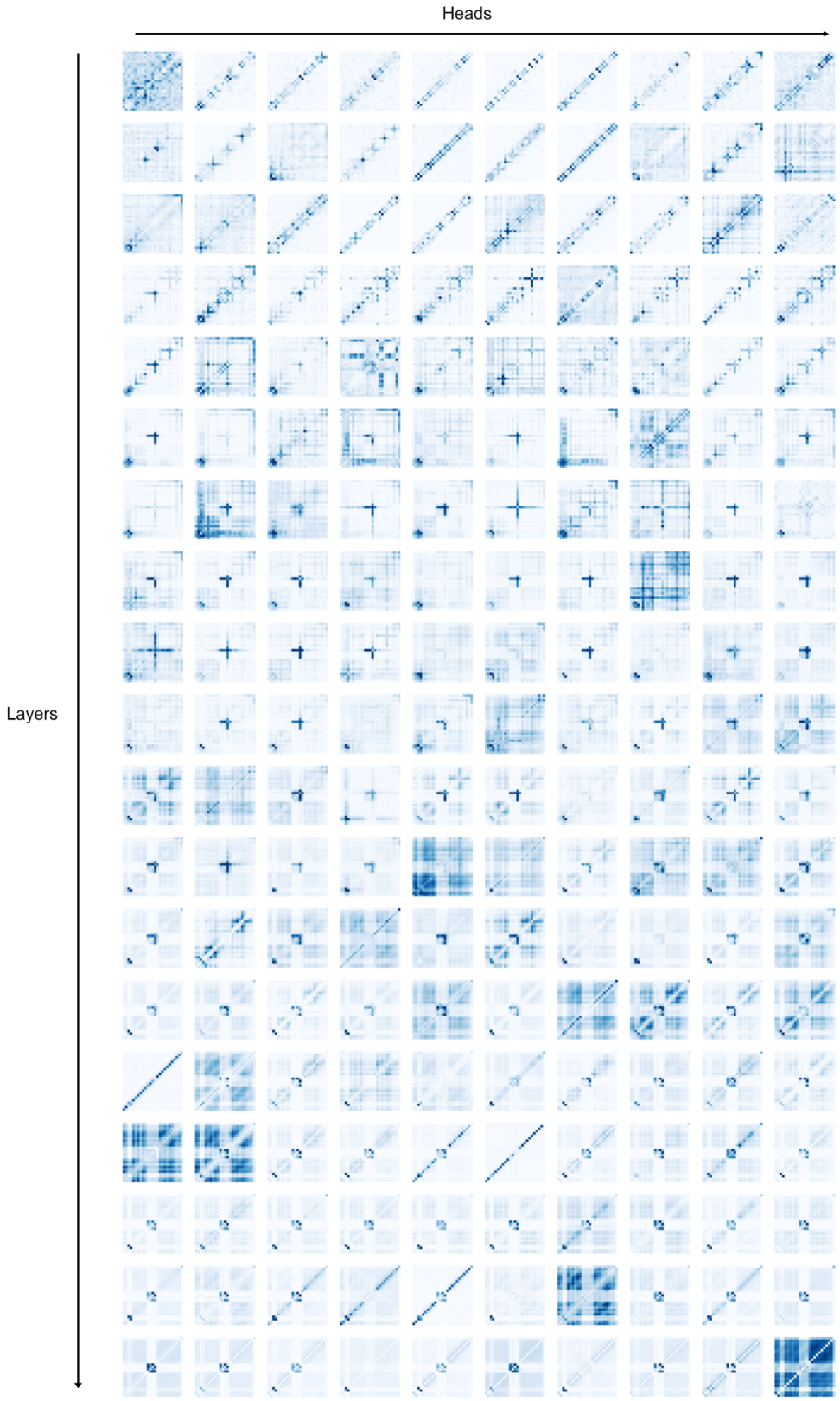

Extended data 5. Visualization of attention heads for a randomly chosen sequence. Increasing layer depth down the figure.

519 **References**
520

521 1. Redfern, O. C., Dessailly, B. & Orengo, C. A. Exploring the structure and function paradigm. *Curr.*
522 *Opin. Struct. Biol.* **18**, 394–402 (2008).
523 2. Jumper, J. *et al.* Highly accurate protein structure prediction with AlphaFold. *Nature* **596**, 583–589
524 (2021).
525 3. Baek, M. *et al.* Accurate prediction of protein structures and interactions using a three-track neural
526 network. *Science* **373**, 871–876 (2021).
527 4. Rives, A. *et al.* Biological structure and function emerge from scaling unsupervised learning to 250
528 million protein sequences. *Proc. Natl. Acad. Sci. U. S. A.* **118**, (2021).
529 5. Elnaggar, A. *et al.* ProtTrans: Towards Cracking the Language of Life's Code Through Self-
530 Supervised Deep Learning and High Performance Computing. *arXiv [cs.LG]* (2020).
531 6. Madani, A. *et al.* Large language models generate functional protein sequences across diverse
532 families. *Nat. Biotechnol.* 1–8 (2023).
533 7. Wright, S. On the roles of directed and random changes in gene frequency in the genetics of
534 populations. *Evolution* **2**, 279–294 (1948).
535 8. Lynch, M. & Conery, J. S. The Origins of Genome Complexity. *Science* **302**, 1401–1404 (2003).
536 9. Cordero, O. X. & Polz, M. F. Explaining microbial genomic diversity in light of evolutionary
537 ecology. *Nat. Rev. Microbiol.* **12**, 263–273 (2014).
538 10. Treangen, T. J. & Rocha, E. P. C. Horizontal transfer, not duplication, drives the expansion of
539 protein families in prokaryotes. *PLoS Genet.* **7**, e1001284 (2011).
540 11. Shapiro, B. J. *et al.* Population genomics of early events in the ecological differentiation of bacteria.
541 *Science* **336**, 48–51 (2012).
542 12. Kountz, D. J. & Balskus, E. P. Leveraging Microbial Genomes and Genomic Context for Chemical
543 Discovery. *Acc. Chem. Res.* **54**, 2788–2797 (2021).
544 13. Miller, D., Stern, A. & Burstein, D. Deciphering microbial gene function using natural language

processing. *Nat. Commun.* **13**, 5731 (2022).

14. Konno, N. & Iwasaki, W. Machine learning enables prediction of metabolic system evolution in bacteria. *Sci Adv* **9**, eadc9130 (2023).
15. Lin, Z. *et al.* Evolutionary-scale prediction of atomic-level protein structure with a language model. *Science* **379**, 1123–1130 (2023).
16. Vaswani, Shazeer & Parmar. Attention is all you need. *Adv. Neural Inf. Process. Syst.*
17. Devlin, J., Chang, M.-W., Lee, K. & Toutanova, K. BERT: Pre-training of Deep Bidirectional Transformers for Language Understanding. *arXiv [cs.CL]* (2018).
18. Hochreiter, S. & Schmidhuber, J. Long short-term memory. *Neural Comput.* **9**, 1735–1780 (1997).
19. Richardson, L. *et al.* MGnify: the microbiome sequence data analysis resource in 2023. *Nucleic Acids Res.* **51**, D753–D759 (2023).
20. Blattner, F. R. *et al.* The complete genome sequence of Escherichia coli K-12. *Science* **277**, 1453–1462 (1997).
21. Jeffery, C. J. Protein moonlighting: what is it, and why is it important? *Philos. Trans. R. Soc. Lond. B Biol. Sci.* **373**, (2018).
22. Miskei, M. *et al.* Fuzziness enables context dependence of protein interactions. *FEBS Lett.* **591**, 2682–2695 (2017).
23. Gherardini, P. F., Wass, M. N., Helmer-Citterich, M. & Sternberg, M. J. E. Convergent evolution of enzyme active sites is not a rare phenomenon. *J. Mol. Biol.* **372**, 817–845 (2007).
24. Ben-Hur, A. & Brutlag, D. Remote homology detection: a motif based approach. *Bioinformatics* **19 Suppl 1**, i26–33 (2003).
25. Bertram, S. *et al.* Methanogenic capabilities of ANME-archaea deduced from ^{13}C-labelling approaches. *Environmental Microbiology* vol. 15 2384–2393 Preprint at https://doi.org/10.1111/1462-2920.12112 (2013).
26. Moran, J. J., House, C. H., Thomas, B. & Freeman, K. H. Products of trace methane oxidation during nonmethyltrophic growth by*Methanosarcina*. *Journal of Geophysical Research* vol. 112

Preprint at https://doi.org/10.1029/2006jg000268 (2007).

27. Shao, N. *et al.* Expression of divergent methyl/alkyl coenzyme M reductases from uncultured archaea. *Commun Biol* **5**, 1113 (2022).

28. Reif, E. *et al.* Visualizing and measuring the geometry of BERT. *Adv. Neural Inf. Process. Syst.* **32**, (2019).

29. Vanni, C. *et al.* Unifying the known and unknown microbial coding sequence space. *Elife* **11**, (2022).

30. Bileschi, M. L. *et al.* Using deep learning to annotate the protein universe. *Nat. Biotechnol.* **40**, 932–937 (2022).

31. Heinzinger, M. *et al.* Contrastive learning on protein embeddings enlightens midnight zone. Preprint at https://doi.org/10.1101/2021.11.14.468528.

32. Egelhofer, V., Schomburg, I. & Schomburg, D. Automatic Assignment of EC Numbers. *PLoS Computational Biology* vol. 6 e1000661 Preprint at https://doi.org/10.1371/journal.pcbi.1000661 (2010).

33. Melo, A. M. P., Bandeiras, T. M. & Teixeira, M. New Insights into Type II NAD(P)H:Quinone Oxidoreductases. *Microbiol. Mol. Biol. Rev.* **68**, 603 (2004).

34. Schirmer, T. C-di-GMP Synthesis: Structural Aspects of Evolution, Catalysis and Regulation. *J. Mol. Biol.* **428**, 3683–3701 (2016).

35. Walsh, D. A., Glass, D. B. & Mitchell, R. D. Substrate diversity of the cAMP-dependent protein kinase: regulation based upon multiple binding interactions. *Curr. Opin. Cell Biol.* **4**, 241–251 (1992).

36. Mittenhuber, G. Phylogenetic analyses and comparative genomics of vitamin B6 (pyridoxine) and pyridoxal phosphate biosynthesis pathways. *J. Mol. Microbiol. Biotechnol.* **3**, 1–20 (2001).

37. Yu, T. *et al.* Enzyme function prediction using contrastive learning. *Science* **379**, 1358–1363 (2023).

38. Ryu, J. Y., Kim, H. U. & Lee, S. Y. Deep learning enables high-quality and high-throughput prediction of enzyme commission numbers. *Proc. Natl. Acad. Sci. U. S. A.* **116**, 13996–14001

(2019).

39. Li, Y. *et al.* DEEPre: sequence-based enzyme EC number prediction by deep learning. *Bioinformatics* **34**, 760–769 (2017).

40. Rogers, A., Kovaleva, O. & Rumshisky, A. A primer in BERTology: What we know about how BERT works. *Trans. Assoc. Comput. Linguist.* doi:10.1162/tacl_a_00349/96482.

41. Vig, J. *et al.* BERTology Meets Biology: Interpreting Attention in Protein Language Models. *arXiv [cs.CL]* (2020).

42. Salgado, H. *et al.* Using RegulonDB, the Escherichia coli K-12 Gene Regulatory Transcriptional Network Database. *Curr. Protoc. Bioinformatics* **61**, 1.32.1–1.32.30 (2018).

43. Ovchinnikov, S., Kamisetty, H. & Baker, D. Robust and accurate prediction of residue-residue interactions across protein interfaces using evolutionary information. *Elife* **3**, e02030 (2014).

44. View article. https://scholar.google.ch/citations?view_op=view_citation&hl=en&user=BA0mI18AAAAJ&sortby=pubdate&citation_for_view=BA0mI18AAAAJ:WF5omc3nYNoC.

45. Guo, J. *et al.* VirSorter2: a multi-classifier, expert-guided approach to detect diverse DNA and RNA viruses. *Microbiome* **9**, 37 (2021).

46. Kaplan, J. *et al.* Scaling Laws for Neural Language Models. *arXiv [cs.LG]* (2020).

47. Kiros, R., Salakhutdinov, R. & Zemel, R. Multimodal Neural Language Models. in *Proceedings of the 31st International Conference on Machine Learning* (eds. Xing, E. P. & Jebara, T.) vol. 32 595–603 (PMLR, 22--24 Jun 2014).

48. Steinegger, M. & Söding, J. MMseqs2 enables sensitive protein sequence searching for the analysis of massive data sets. *Nat. Biotechnol.* **35**, 1026–1028 (2017).

49. Lin, Z. *et al.* Evolutionary-scale prediction of atomic level protein structure with a language model. *bioRxiv* 2022.07.20.500902 (2022) doi:10.1101/2022.07.20.500902.

50. Liu, Y. *et al.* RoBERTa: A Robustly Optimized BERT Pretraining Approach. *arXiv [cs.CL]* (2019).

51. Huang, Z., Liang, D., Xu, P. & Xiang, B. Improve Transformer Models with Better Relative Position

Embeddings. *arXiv [cs.CL]* (2020).

52. Loshchilov, I. & Hutter, F. Decoupled Weight Decay Regularization. *arXiv [cs.LG]* (2017).
53. Tierrafría, V. H. *et al.* RegulonDB 11.0: Comprehensive high-throughput datasets on transcriptional regulation in Escherichia coli K-12. *Microb Genom* **8**, (2022).
54. Buchfink, B., Xie, C. & Huson, D. H. Fast and sensitive protein alignment using DIAMOND. *Nat. Methods* **12**, 59–60 (2015).
55. Suzek, B. E., Huang, H., McGarvey, P., Mazumder, R. & Wu, C. H. UniRef: comprehensive and non-redundant UniProt reference clusters. *Bioinformatics* **23**, 1282–1288 (2007).
56. Li, W., Jaroszewski, L. & Godzik, A. Clustering of highly homologous sequences to reduce the size of large protein databases. *Bioinformatics* **17**, 282–283 (2001).